JOURNAL OF MATERIALS SCIENCE 27 (1992) 1528–1536

Effect of gas phase on SiC and Si_3N_4 formations from SiO_2

H. WADA, L. WANG
Department of Materials Science and Engineering, University of Michigan, Ann Arbor, MI 48109, USA

During the synthesis of SiC, Si_3N_4 and sialon whiskers by carbothermal reduction of SiO_2, a localized formation of amorphous phases or Si_2N_2O powders was observed beneath these whiskers. Because these whiskers were formed by the vapour/solid mechanism, the controlling gas phase was of primary importance to obtain whiskers of tailored morphology and chemistry. To elucidate the effect of the gas phase composition on the reaction mechanisms of SiC and Si_3N_4, the oxygen partial pressure was measured during the synthesis with a ZrO_2 solid electrolyte. The carbothermal reduction of SiO_2, as well as evolution of gases, were accelerated by a formation of a molten fluorosilicate with an auxiliary halide bath. The oxygen partial pressure steadily increased with increasing temperature and reached a maximum level of 10^{-11}–10^{-12} atm in the early stage of reaction at 1623 K, then decreased again towards the end of reaction in both cases. Effects of the gas phase on the SiC and Si_3N_4 formations were not the same: p_{CO} and p_{CO_2} and their ratio were important factors in the SiC formation, while the higher p_{O_2} formed an oxynitride phase in the Si_3N_4 formation.

1. Introduction

Effects of gas phase on phase stability were recognized during ceramic whisker synthesis by the carbothermal reduction of SiO_2 [1–10]. Because ceramic whiskers such as SiC, Si_3N_4 and sialon were synthesized by the vapour/solid mechanism (VS mechanism), it was expected that the control of gas composition would be of primary importance in obtaining whiskers of tailored morphology and chemistry. During the ceramic whisker synthesis it became clear that the gas phase composition, particularly partial pressures of oxygen and carbon monoxide, and also a flow rate of nitrogen, had a decisive effect on reaction products [3, 4]. Other gas species, for instance SiO, were formed during the carbothermal reduction of SiO_2, and its partial pressure was closely related to those of oxygen and carbon monoxide in the system. The oxygen partial pressure has been measured during Si_3N_4 whisker synthesis by using a ZrO_2 solid electrolyte and briefly reported [1]. More accurate gas phase analysis over a wider range of temperatures, however, became necessary to understand the complicated reaction mechanisms of SiC and Si_3N_4/Si_2N_2O formations, which involved a molten salt bath. The effect of gas phase composition was reported by Milewski *et al.* [7]. They examined the effect of gas composition in their SiC whisker formation by the vapour/liquid/solid mechanism (VLS mechanism) and proposed an identification chart for SiC growth conditions.

A localized formation of fine Si_2N_2O or O′-sialon powder was persistently observed during our Si_3N_4 synthesis with nitrogen gas [2, 6], while a localized amorphous phase remained in SiC synthesis under argon gas [3]. Although this localized formation of oxygen-containing phases beneath the whiskers was related thermodynamically to a higher p_{O_2} and $[p_{SiO}/p_{N_2}]$ ratio in nitride whisker synthesis [2, 6], a more detailed analysis of the gas phase during the reduction of SiO_2 became necessary to gain insight into the effect of gas phase on the whisker and powder formation.

Oxygen partial pressure was measured by a ZrO_2 solid electrolyte during both the carbide and the nitride syntheses. Experimental results showed that the oxygen partial pressure changed in a range from 10^{-20}–10^{-11} atm during the reaction. The purpose of this paper is to relate these experimental results to the similarities and the differences between the carbide and nitride formations to understand complicated reaction mechanisms.

2. Experimental procedure

2.1. Reaction system

An experimental arrangement is shown in Fig. 1. A mixture of SiO_2/Carbon/$3NaF \cdot AlF_3$ in 1/3/0.3 mole ratio or SiO_2/C/NaF in 1/3/1 mole ratio, was placed in a graphite reaction tube. The ratio of Si/C/Na was kept as 1/3/1 for both cases in this way. The total weight of these starting materials was kept in three levels: 3.2, 9.6 and 12.8 g. Furnace temperature was increased at a rate of $\simeq 8\,^{\circ}C\,min^{-1}$ to the reaction temperature, 1623 K; the regular reaction time was 8 or 9 h at 1623 K, but two selected runs, one for nitride formation and the other for carbide formation, were interrupted after only 2 and 3 h, respectively. The

0022–2461

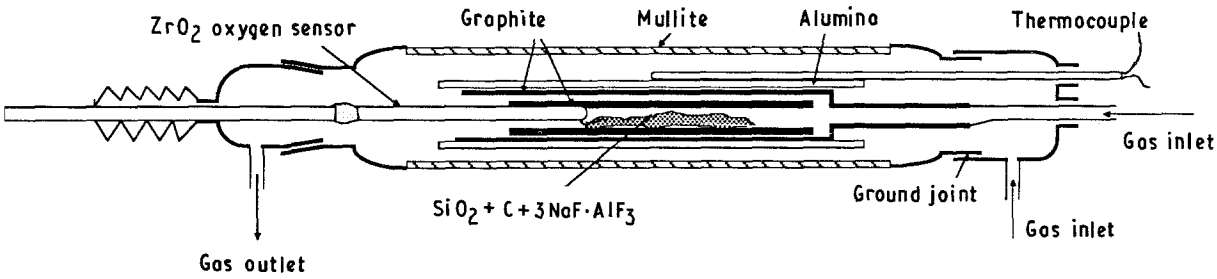

Figure 1 Apparatus for e.m.f. measurement.

flowing gases were Ar–5% H_2 and N_2–5% H_2 for the SiC and Si_3N_4 whisker formation, respectively. The high-purity flowing gases were further purified by $Mg(ClO_4)_2$ columns. The gas flow rate was in a range 45–150 $cm^3\,min^{-1}$, which was controlled by a Matheson 602 type flow meter calibrated for each gas by the bubble method.

2.2. Oxygen partial pressure measurements

Oxygen partial pressure was measured for selected runs using a ZrO_2 sensor. To minimize the detrimental effect of a highly reducing atmosphere caused by high carbon activity and a halide auxiliary bath, the sensor was arranged to be as movable as possible with a flexible connector; it was kept at the lower temperature area of the furnace while e.m.f. was not being measured, and then it was inserted into the reaction region when e.m.f. was measured. The direction of the following gas was changed to protect the ZrO_2 tube when e.m.f. was not being measured. The e.m.f. was measured with a digital voltmeter at a certain interval during heating and continued at the reaction temperature 1623 K.

2.2.1. Solid electrolyte cell

Fig. 2 shows the solid electrolyte cell arrangement. A one-end closed ZrO_2 tube, stabilized either by CaO or MgO, was filled with a Mo/MoO_2 powder mixture with the weight ratio $Mo:MoO_2 = 1:3$ or 9:1. The mixture and molybdenum wire inside the electrolyte cell, and molybdenum or iridium wires outside were a reference electrode and a working electrode, respectively. The galvanic cell was formed as

$$Mo/Mo\text{–}MoO_2/ZrO_2(CaO \text{ or } MgO)/O_2 \text{ (in reaction)}/Mo \text{ or } Ir \quad (1)$$

The corresponding reaction for the cell is therefore

$$O_2(Mo/MoO_2) = O_2 \text{ (in reaction)} \quad (2)$$

The oxygen partial pressure, p_{O_2}, was calculated by assuming that the ionic conductivity is unity as

$$\ln p_{O_2} \text{ (in reaction)} = -4FE/RT + \ln p_{O_2}(Mo/MoO_2) \quad (3)$$

where F is the Faraday constant and E the e.m.f. values measured and R the gas constant. The temperature, T, was measured by a built-in Pt/Pt–10%Rh thermocouple. The reference oxygen partial pressure,

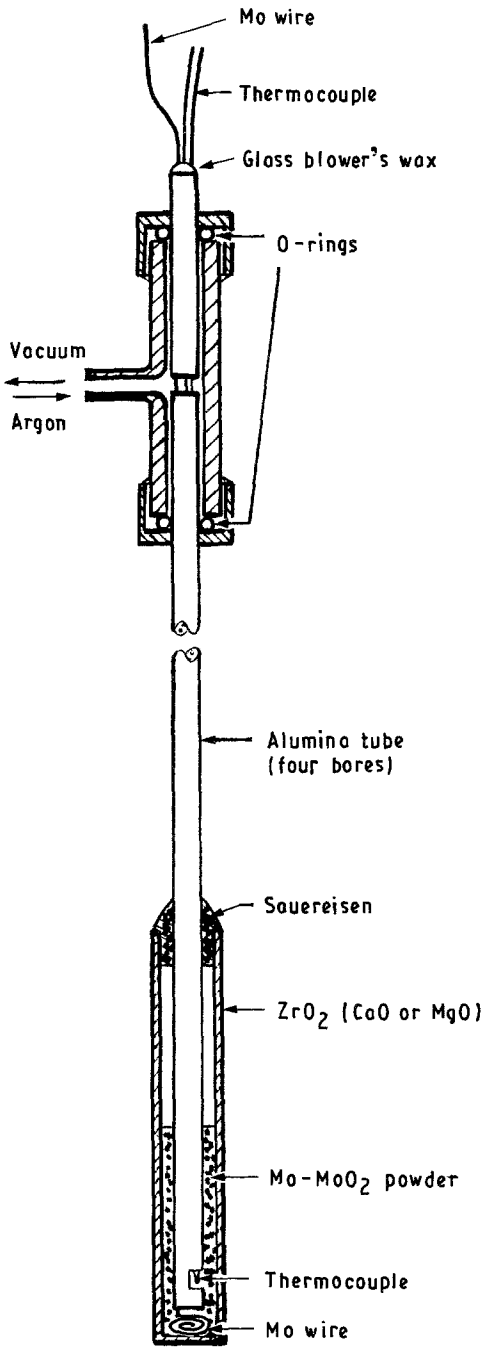

Figure 2 Mo–MoO_2 reference electrode.

$p_{O_2}(Mo/MoO_2)$, was determined against air ($p_{O_2} = 0.2093$ atm) for the reaction $Mo + O_2 = MoO_2$ as

$$\log p_{O_2} = -29\,519/T + 8.46 \quad (4)$$

Equation 4 is in good agreement with our previous

measurement [11] and those reported in the literature [12–14].

2.3. Characterization

The reaction products were separated into two parts, whiskers and powders beneath the whiskers, after the reaction. Each part was identified by X-ray diffraction (XRD) with pure silicon as an internal standard. The morphology and composition were investigated with a scanning electron microscope (SEM, Hitachi S-520) and transmission electron microscope (TEM, Jeol 2000FX), respectively.

3. Results and discussion

3.1. Experimental results

Logarithms of p_{O_2} values which were measured during heating are plotted as a function of $1/T$ in Figs 3 and 4 for the SiC and Si_3N_4 whiskers formation, respectively. The equilibrium oxygen partial pressures of the reaction $C + 1/2\,O_2 = CO$ are also shown in both Figs 3 and 4 by dotted lines for $p_{CO} = 1$–0.01 atm. The p_{O_2} increased gradually with increasing furnace temperature up to 1373 K, and then it increased rapidly to its maximum when the temperature reached the reaction temperature of 1623 K. The p_{O_2} started to decrease after the sample was held at 1623 K for several hours in both reactions. Arrows in Figs 3 and 4 indicate these decreases in p_{O_2} in isothermal holding at 1623 K. A typical change in p_{O_2} during this isothermal holding at 1623 K, is shown in Fig. 5.

The p_{O_2} in the heating period is close to the equilibrium value for $p_{CO} = 0.1$ atm up to 1373 K. The p_{O_2} departs from the equilibrium lines thereafter, increasing to the maximum level of 10^{-11}–10^{-12} atm at 1623 K. During the holding at 1623 K, the p_{O_2} gradually reached to the level corresponding to p_{CO} of about 0.1 atm.

The time–temperature range in which the p_{O_2} is

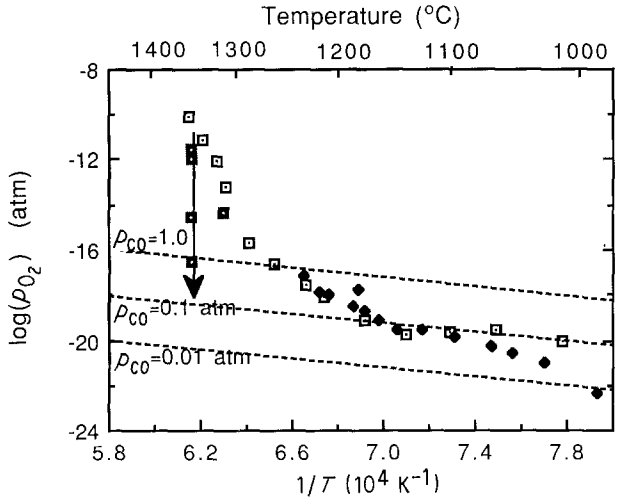

Figure 3 Changes in log p_{O_2} during SiC formation. Run: (□) 6, (◆) 32, (■) 33; (---) $C + 1/2O_2 = CO$.

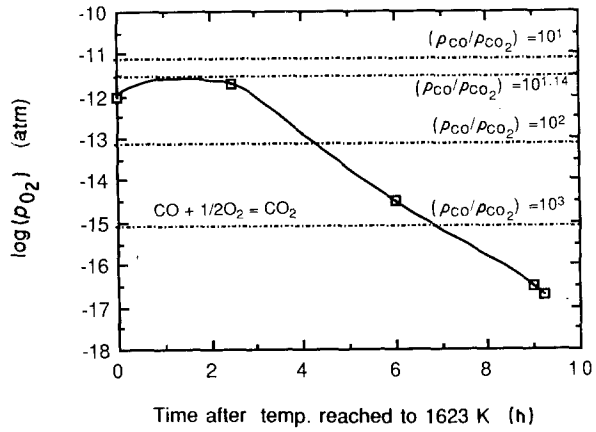

Figure 5 Typical p_{O_2} profile with reaction time at 1623 K with argon gas. Argon flow rate = 45 cm^3 min^{-1}; $SiO_2/3NaF \cdot AlF_3$ = 3:1 (mole ratio).

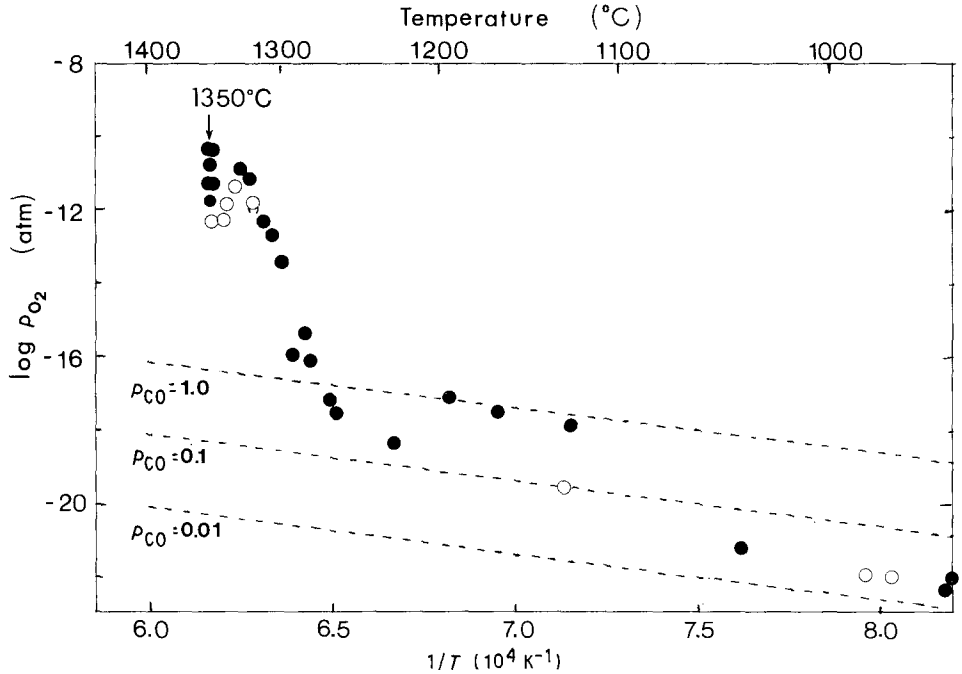

Figure 4 Changes in log p_{O_2} during Si_3N_4 formation. Run: (○) 29, NaF, (●) 35, Na_3AlF_6; (---) $C + 1/2O_2 = CO$.

higher than the value of $C/O_2/CO$ equilibrium corresponds to the range in which the carbothermal reaction of silica takes place. The only source of oxygen in this system is SiO_2, then the oxygen detected in this measurement was produced as a result of two parallel reactions:

(1) the formation of oxygen and carbon dioxide as a result of reactions between SiO_2, carbon and halides, and

(2) the reaction of oxygen and carbon dioxide with carbon to reach the $C/O_2/CO$ equilibrium. The observed high p_{O_2} indicates that Process 1 above dominates in this time–temperature range rather than Process 2. Both SiC and Si_3N_4 formations show the same p_{O_2} deviation because the reaction of SiO_2, carbon and halide to form oxygen are common in both systems.

The high p_{O_2} indicates a very active carbothermal reduction of SiO_2 taking place in the molten halide bath. The reaction in the bath has been discussed previously [4] in connection with a formation of molten fluorosilicates. The enhancing effect of molten fluorosilicates was reported by Saito *et al.* [8–10]. They examined the effect of several fluorides on the Si_3N_4 whisker formation from SiO_2. They concluded that the fluorides which formed molten fluorosilicates with SiO_2 (for example, NaF, CaF_2 and $3NaF \cdot AlF_3$) enhanced reaction, while others which formed no melt with SiO_2 (for example, AlF_3) showed little effect on the reaction. Figs 3 and 4 show that the increase in p_{O_2} started at about 1373 K. This temperature seems to correspond to the beginning of SiO_2 dissolution into the molten halide; the melting points of $3NaF \cdot AlF_3$ and NaF are 1282 and 1268 K, respectively.

Increases in the amount of exhaust gas were also observed around these melting points. The exhaust was collected in a bubbler that contained a saturated $PbCl_2$ solution of pH = 4 [4]. Fluorine in the exhaust was precipitated as PbClF resulting in higher acidity in the solution. A typical change of the solution pH during heating is shown in Fig. 6. (□). The reaction time is taken to be zero when the furnace temperature reached 1273 K. The pH decreased rapidly between 1273 and 1373 K, and remained almost unchanged thereafter. If SiO_2 was replaced by silicon as the starting material, the pH changed much slower as seen in Fig. 6, but eventually it reached the same level as that in the SiO_2 case. Several analyses of vaporized and condensed materials in the gas outlet tube suggested that the major species vapourized from the molten fluorosilicate was $NaF \cdot AlF_3$, which then solidified mainly as $3NaF \cdot AlF_3$ in cooler parts of the gas outlet tube. Combining these facts with the observation that the carbon consumption was only one-quarter of that in the SiO_2 [4], it can be concluded that SiO(g) and probably CO were produced by the reduction of fluorosilicate, and evolved from the melt, while fluorine evolved probably as F_2. Sodium and aluminium were not detected in the $PbCl_2/PbClF$ solution by an atomic absorption spectroscopy.

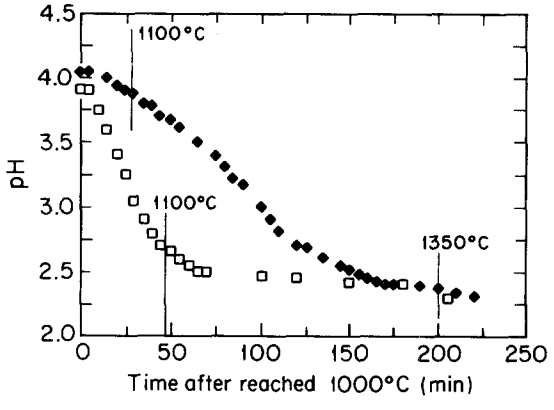

Figure 6 Typical changes in pH of $PbCl_2$ solution by exhaust during silicon nitride formation. (□) SiO_2, (◆) Si.

The thermodynamic nature of the molten sodium–aluminium-fluorosilicate is largely unknown at present, but it is well established that the viscosities of metal oxides can be reduced by an addition of fluorides. For instance, Kato and Minowa [15] reported a comprehensive study on the relationship between viscosity and electrical conductivity of molten slags. In the study, they reported that fluorides reduced the viscosity of Al_2O_3(14)–SiO_2(43)–CaO(43) slag; 20 mol % NaF, CaF_2 and MgF_2 reduced the viscosity of the slag from the order of 10 poise to the order of 0.4, 0.8 and 2 poise, respectively, at 1673 K. As a result of the reduced viscosity, the reaction between SiO_2 and carbon as well as evolution of resulting gases would be greatly enhanced in the present work.

To determine the effect of fluorosilicate formation and gas phase composition on both SiC and Si_3N_4 reactions, two sets of samples with different reaction times were examined by XRD as well as SEM for each reaction. Fig. 7a compares XRD patterns of two samples obtained at the bottom of charged materials after 3 and 9 h reaction times for SiC with flowing Ar–5% H_2. A high-purity silicon was added as an internal standard. The 3 h sample consists of an amorphous phase and SiC phase, while the 9 h sample contained crystallized aluminium–sodium-silicate in addition to the SiC and amorphous phases. The same comparison is made in Fig. 7b for Si_3N_4 formed with flowing 1 atm N_2–5% H_2. The 2 h sample shows a pattern remarkably similar to the 3 h SiC sample shown in Fig. 7a, except O′-sialon is formed under nitrogen gas instead of SiC. After 8 h reaction, β′ and x phases are formed in addition to O′-sialon and little amorphous phase remains.

The SEM and TEM observations are

SiC
- 3 h sample – powder + short SiC whiskers
- 9 h sample – powder + short SiC whiskers

Si_3N_4
- 2 h sample – round shaped, thin, very fine O′-sialon powders with average diameter less than 0.5 μm
- 8 h sample – O′-, β′-sialon powders and x phase powders. No changes are observed in their shapes from those in the 2 h sample.

The differences seen in Fig. 7a and b are probably related to a distinctive difference in the solubilities of aluminium in SiC and Si_3N_4. The lowest atomic ratio Si/Al measured for β′-sialon powder in this study was Si/Al = 1.2, while it was Si/Al = 49 for SiC. Under

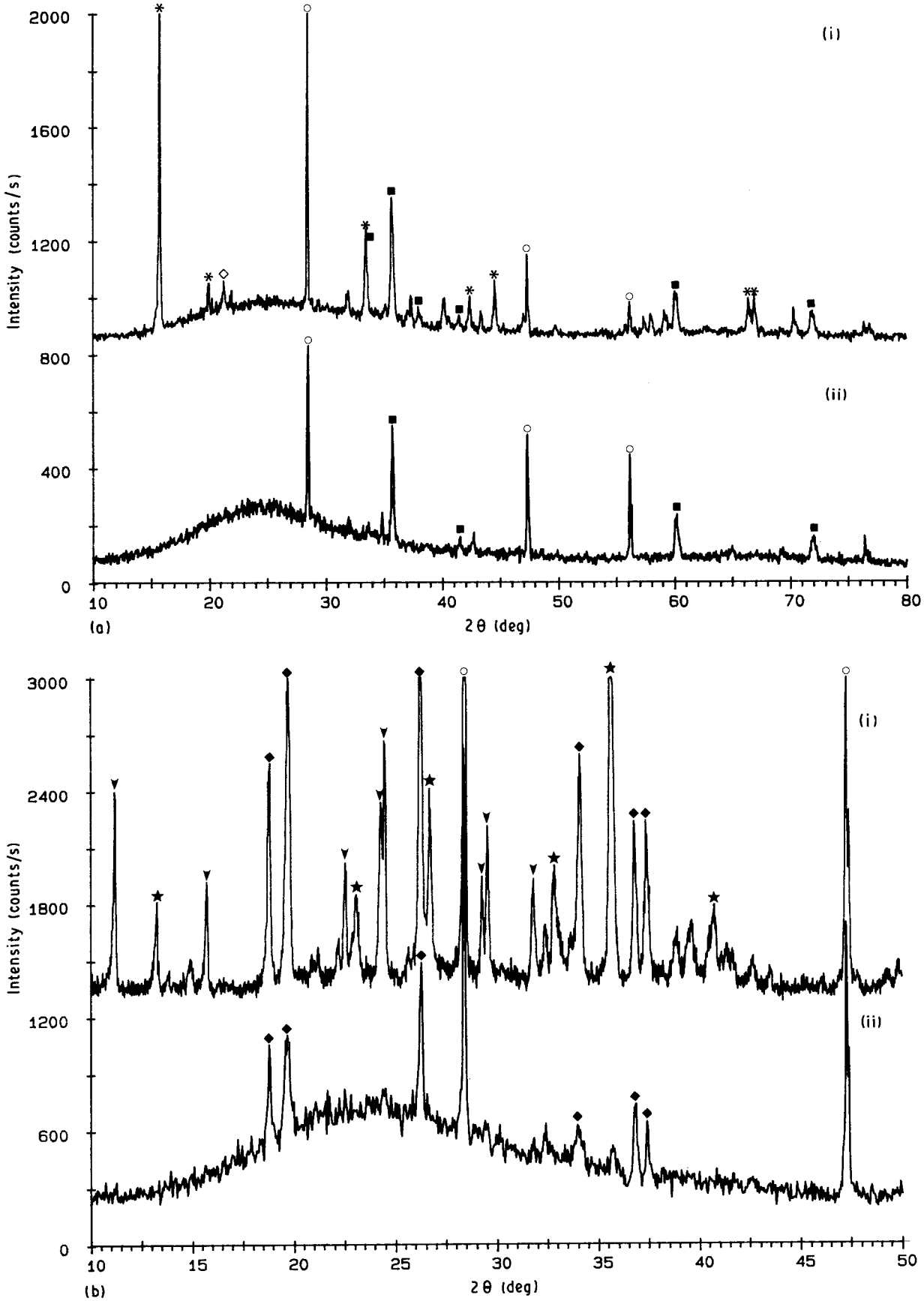

Figure 7 XRD patterns of the sample formed in the bottom of a powder bed in (a) SiC formation, (i) $t = 9$ h, $T = 1623$ K, argon flow rate $= 45\ cm^3\ min^{-1}$, (ii) $t = 3$ h, $T = 1623$ K, argon flow rate $= 45\ cm^3\ cm^{-1}$. and (b) Si_3N_4 formation, (i) $t = 8$ h, $T = 1623$ K, nitrogen flow rate $= 100\ cm^3\ min^{-1}$, (ii) $t = 2$ h, $T = 1623$ K, nitrogen flow rate $= 100\ cm^3\ min^{-1}$. (a) (■) SiC, (*) $NaAl_{11}O_{17}$, (◇) $NaAlSiO_4$, (○) Si (standard); (b) O′-sialon (★) β′-sialon, (▼) X′-phase, (○) Si (standard).

argon gas flow, therefore, more aluminium and probably oxygen remained in the fluorosilicate, while it was incorporated into β′-sialon under nitrogen gas. Composition of the remaining fluorosilicates showed that it moved toward less silicon, sodium and fluorine with reaction time under argon gas. Because the melting point of the fluorosilicate rises as its composition moves toward higher aluminium content, sodium–

aluminium-silicates would probably become similar to albite, napheline and carnegieite toward the end of 8–9 h reaction under argon gas. In fact, XRD of powders sampled just beneath the SiC whiskers shows similar patterns to aluminium–sodium–aluminium silicate. These silicates and amorphous material could easily be eliminated by either replacing $3NaF \cdot AlF_3$ with NaF or raising the reaction temperature [3].

Under nitrogen gas, on the other hand, aluminium as well as oxygen dissolved in Si_3N_4 during the synthesis and formed sialon, $Si_{6-x}Al_xN_{8-x}O_x$. Neither amorphous phase nor aluminium silicate phase was detected in powders sampled just beneath the β'-Si_3N_4 whiskers after 8 h reaction at 1623 K.

3.2. Reaction mechanism

It has been shown in our previous reports that both SiC and Si_3N_4 whiskers were formed by the gas/solid reaction [1–6]: the silicon precursor was a SiO gas which reacted with carbon monoxide or nitrogen to form SiC or Si_3N_4 whiskers most likely on carbon powder as the substrate. A reaction of SiO(g) with solid carbon was not likely to contribute to whisker growth because a necessary diffusion of solid carbon to the growth site on the whisker tip should be slow; however, it could be involved in the powder/amorphous SiC formation in the bottom area of powder bed. Phases in the Si–N–O system are more complicated than the Si–C system because of the presence of silicon oxynitrides such as Si_2N_2O and O′-sialon. These oxinitrides provide more insight into reaction mechanisms.

Both Si_2N_2O and O′-sialon are more stable than Si_3N_4 at the higher oxygen potential [16–20] as well as at the higher $[p_{SiO}/p_{N_2}]$ ratio if oxygen partial pressure is fixed [2]. In the present work, the stable phase was Si_2N_2O/or O′-sialon during the first 2 h reaction with nitrogen, in which the oxygen partial pressure was usually in the range $p_{O_2} = 10^{-11}$–10^{-12} atm. Because Si_2N_2O was the only crystalline phase formed in this period, this high oxygen partial pressure is taken as in equilibrium with Si_2N_2O. The reaction then can be expressed as

$$Si_2N_2O + \tfrac{1}{2}O_2(g) = 2SiO(g) + N_2(g) \quad (5)$$

$$\log K_5 = \log \{p_{SiO}^2 p_{N_2} / a_{Si_2N_2O} p_{O_2}^{1/2}\} = -23089/T + 15.20 \text{ [21]} \quad (6)$$

In this calculation $a_{Si_2N_2O}$, a_{SiO_2}, a_{SiC} and a_C are referred to the solid Si_2N_2O, cristobalite, SiC(β) and graphite, respectively. A partial pressure of SiO is estimated from Equation 6 for $a_{Si_2N_2O} = 1$, $p_{N_2} = 1$ and $p_{O_2} = 10^{-11.5}$ atm as, $\log p_{SiO} = -2.388$.

The formation of Si_2N_2O was also the gas/solid reaction and expressed by the following reaction [4]:

$$2SiO(g) + CO(g) + N_2(g) = Si_2N_2O + CO_2(g) \quad (7)$$

$$\log K_7 = \log \{a_{Si_2N_2O} p_{CO_2} / p_{SiO}^2 p_{CO} p_{N_2}\} = 3.64 \text{ at } 1623 \text{ K [16]} \quad (8)$$

Because $a_{Si_2N_2O} = 1$ and $p_{N_2} = 1$ atm, the CO/CO_2 ratio can be estimated for this particular period of nitride formation. Substituting the estimated value of p_{SiO} into K_7, (p_{CO}/p_{CO_2}) is estimated as 13.7. When Si_2N_2O was the only crystalline phase, then the CO/CO_2 ratio is low and the partial pressures of oxygen, carbon monoxide and carbon dioxide were controlled by the following reaction:

$$CO(g) + \tfrac{1}{2}O_2(g) = CO_2(g) \quad (9)$$

$$\log K_9 = 14577/T - 4.388 \text{ [21]} \quad (10)$$

Because those high p_{O_2} and low p_{CO}/p_{CO_2} ratios were common in both carbide and nitride formations, they were generated by one common reaction: the carbothermal reduction of SiO_2. There are many publications on the carbothermal reduction of silica and the application to SiC as well as Si_3N_4 powder synthesis; the subject was recently summarized by Biernacki and Wotzak [22], and the formation of nitride powder was discussed by Cannon and Zhang [23], Lee and Cutler [24] and Mori *et al.* [25]. As replacing SiO_2 with silicon did not produce Si_3N_4, SiO(g) and probably CO(g) were most likely generated from the carbothermal reduction of SiO_2 which formed fluorosilicate. An additional run was performed to confirm the generation of CO(g): the flowing gas was replaced by Ar–10% CO gas for SiC formation. The gas flow rate was 45 $cm^3 min^{-1}$ and the other reaction parameters were kept the same. At the end of a 9 h reaction, neither SiC whiskers nor powders were formed, and a fluorosilicate was the only phase present in the reaction tube. Also the reduction of pH in a $PbCl_2$ solution was much slower than those with the regular Ar–5% H_2 gas. The addition of CO in the gas deterred the decomposition of fluorosilicate as well as the gas evolution.

Although the vapourizing $3NaF \cdot AlF_3$ might contain silicon, a major decomposition of SiO_2 can be expressed as

$$SiO_2(\text{fluorosilicate}) + C = SiO(g) + CO(g) \quad (11)$$

Because CO/CO_2 was controlled by Equation 9, the whole reaction could be expressed for the early stage of reaction as

$$SiO_2(\text{fluorosilicate}) + C + \tfrac{1}{2}O_2(g) = SiO(g) + CO_2(g) \quad (12)$$

$$\log K_{12} = \log \{p_{SiO} p_{CO_2} / a_{SiO_2} a_C p_{O_2}^{1/2}\} = -20684/T + 13.11 \text{ [21]} \quad (13)$$

It is necessary to mention that there was a possible presence of more free oxygen in the molten fluorosilicate compared with the molten silicate, because Reaction 12 could involve $\underline{O}$ (fluorosilicate) = $1/2O_2(g)$. In this calculation, however, the activity of oxygen in molten fluorosilicate is regarded as $a_O = p_{O_2}^{1/2}$. Substituting the measured p_{O_2} and the estimated p_{SiO}, and assuming $a_{SiO_2} = a_C = 1$, a possible partial pressure of CO_2 is calculated as $p_{CO_2} = 0.001$ atm, and then $p_{CO} = 0.014$ atm. Although a_{SiO_2} is assumed as unity in the calculation, the solid cristobalite, standard state of a_{SiO_2}, was never detected in this work. Therefore, a_{SiO_2} might be less than unity in the molten fluorosilicate, and as a result the phase boundary between Si_2N_2O

and SiO_2 might be shifted to higher oxygen partial pressure.

In the early stage of nitride formation, the gas phase composition was high in oxygen, SiO and CO_2 as a result of an enhanced reduction of SiO_2 as well as gas evolution. This gas composition then affected the phase stability of the Si–N–C–O system and the Si_2N_2O/O′-sialon was formed as the major phase. However, these solid phases became further from the stable phase as the reaction proceeded, resulting in less evolution of gases and increasing viscosity of the molten fluorosilicate. When the p_{O_2} decreased while a_C was kept unchanged with excess carbon, β′-Si_3N_4 or β′-sialon became more stable than those oxynitrides [20]. The fact that the relative amounts of O′ to β′ in the bottom area of the powder bed decreased with reaction time, as seen in Fig. 6b, suggests that the majority of O′-sialon might eventually be decomposed/transformed to β′-phase. In fact, all O′-sialon powder disappeared after annealing at 1623 K under the condition of $p_{N_2} = 1$ atm and $a_C = 1$ [26].

The effect of the gas phase composition is more difficult to elucidate on SiC formation because the system has only one phase, SiC. SiC could be formed by the following two reactions:

$$SiO(g) + 2C = SiC(\beta) + CO(g) \quad (14)$$

$$\log K_{14} = \log \{a_{SiC} p_{CO} / p_{SiO} a_C^2\} \quad (15)$$

and

$$SiO(g) + 3CO(g) = SiC(\beta) + 2CO_2(g) \quad (16)$$

$$\log K_{16} = \log \{a_{SiC} p_{CO_2}^2 / p_{SiO} p_{CO}^3\} \quad (17)$$

Free energy change is lower for Reaction 14 but Reaction 16 is required for the whiskers growth in the sample of 3 h reaction. It implies that both reactions might occur in the early stage of carbide formation. Reaction 14 generates high CO: an estimated partial pressure of CO is $\log p_{CO} = -0.0914$ when $\log p_{SiO} = -2.388$, while Reaction 16 requires high p_{CO}/p_{CO_2} ratio such as $p_{CO}/p_{CO_2} = 1.1 \times 10^4$ and 3.2×10^4 or approximately $p_{O_2} = 10^{-18}$ atm, for $p_{CO} = 0.1$ and 0.01, respectively. It was observed that several short SiC whiskers grew in the ⟨1 1 1⟩ direction from a large chunk of SiC [3]. This fact may suggest that SiC was formed by Equation 14 at first, which generated CO, and then whiskers were formed by Equation 16 as the reaction proceeded.

3.3. Supersaturation

To grow whiskers, a certain degree of supersaturation in the gas phase is required. Supersaturation is a ratio

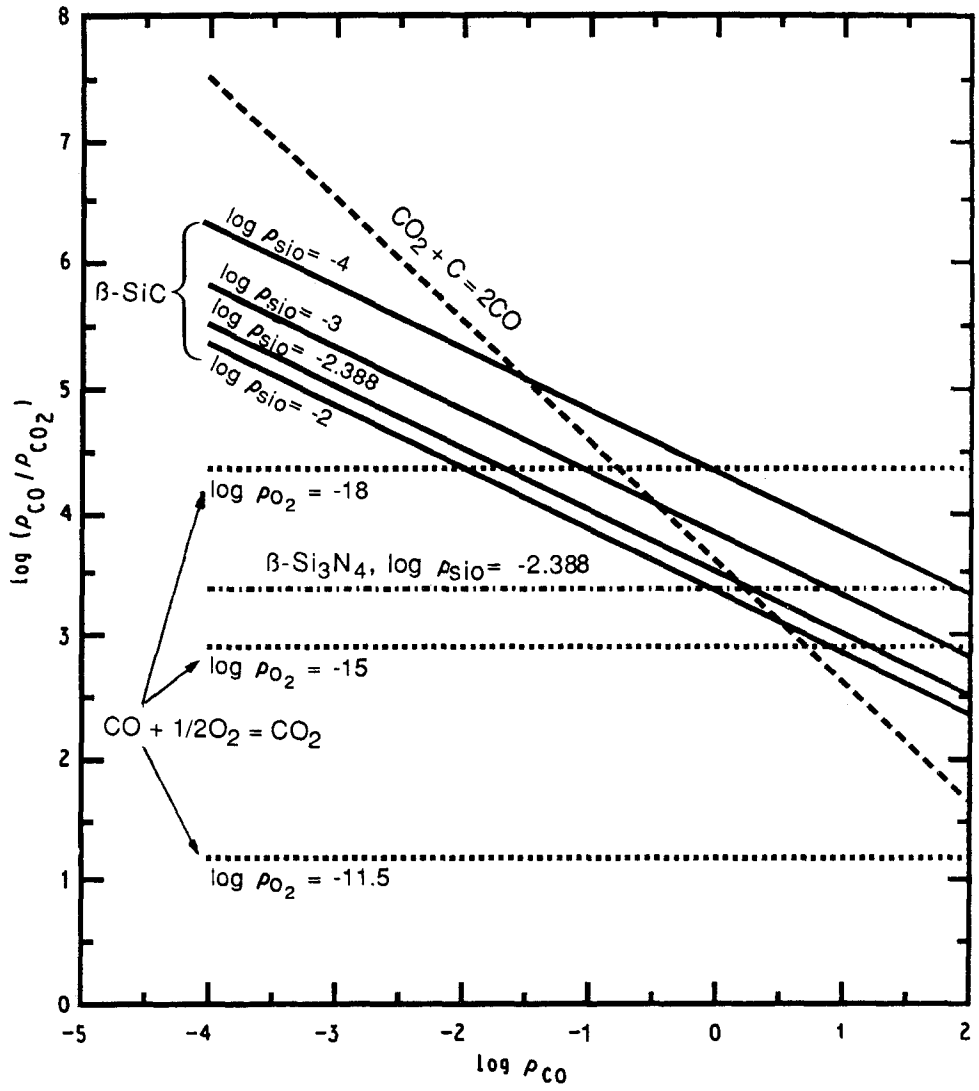

Figure 8 Effect of CO, CO_2 and O_2 partial pressures on supersaturations of SiC and Si_3N_4 formations.

of real gas composition versus one in equilibrium. The degrees of supersaturation are estimated for SiC and Si_3N_4 whisker formation at 1623 K as follows:

SiC. The supersaturation ratio can be expressed for Reaction 16 as

$$\log\{(p_{SiO}p_{CO^3}/p_{CO_2^2})/(p_{SiO}p_{CO^3}/p_{CO_2^2})eq\} = \log p_{SiO} + 3\log p_{CO} - 2\log p_{CO_2} - 4.653 \quad (18)$$

where $(p_{SiO}p_{CO^3}/p_{CO_2^2})_{eq}$ is a product of partial pressures in equilibrium, which is equal to $1/K_{16}$ when $a_{SiC} = 1$.

Si_3N_4. Whisker formation was identified as the gas/solid reaction as follows [4]:

$$3SiO(g) + 3CO(g) + 2N_2(g) = Si_3N_4(\beta) + 3CO_2(g) \quad (19)$$

$$\log K_{19} = \log\{a_{Si_3N_4}p_{CO_2^3}/p_{SiO^3}p_{CO^3}p_{N_2^2}\} = -2.925 \text{ at } 1623 \text{ K [16]} \quad (20)$$

The ratio then can be written for $p_{N_2} = 1$ atm

$$\log\{(p_{SiO^3}p_{CO^3}/p_{CO_2^3})/(p_{SiO^3}p_{CO^3}/p_{CO_2^3})_{eq}\} = 3\log p_{SiO} + 3\log p_{CO}/p_{CO_2} - 2.925 \quad (21)$$

Comparing Equations 18 and 21 it is clearly shown that p_{CO} and p_{CO_2} have a more substantial effect on the SiC whisker formation than on that of the Si_3N_4. The relationships are compared in Fig. 8. To form SiC whiskers when $\log p_{SiO} = -2.388$ and $\log p_{CO} = -1.84$, the p_{CO}/p_{CO_2} ratio in the gas phase should be higher than $\log p_{CO}/p_{CO_2} = 4.4$. SiC whiskers grew in the present work with only 3 h reaction time, because the p_{CO}/p_{CO_2} ratio reached higher than this critical value. It indicates that Reaction 14 generated CO(g), and then SiC whiskers were formed by Reaction 16. To grow β-type Si_3N_4 whiskers, on the other hand, p_{CO} has little effect compared with p_{O_2}. When $\log p_{O_2} = -11.5$ and $\log p_{SiO} = -2.388$, β-type Si_3N_4 whisker would not grow because the p_{CO}/p_{CO_2} ratio in the gas phase was much lower than the required value shown with a dashed/dotted line in Fig. 8. Because the required p_{CO}/p_{CO_2} ratio increases with decreasing p_{SiO}, β-type Si_3N_4 whisker would not grow until either p_{O_2} became very low or p_{CO}/p_{CO_2} became high enough, like those of the CO_2/C/CO reaction shown in Fig. 8.

It can be concluded that the effect of a gas phase on the reaction mechanism is not the same for β-SiC and β-Si_3N_4 formations. The reaction mechanism in nitride formation is affected by the high oxygen partial pressure, and it is affected by the partial pressures of CO and CO_2 in the carbide formation.

4. Conclusion

The carbothermal reduction of SiO_2 was clearly accelerated by the application of a halide bath in the present process resulting in high partial pressures of SiO and O_2 in the early stage of reaction at 1623 K. The oxygen partial pressure reached the maximum level of 10^{-11}–10^{-12} atm then decreased again toward the end of reaction. The patterns in the changing p_{O_2} were similar in both SiC and Si_3N_4 formations. The localized higher partial pressures of oxygen and SiO generated from the molten fluorosilicate could affect both phase stability and morphology of carbide and nitride in the bottom area of the powder bed. However, the effect of gas composition is different in the SiC and Si_3N_4 formations.

Under argon gas, SiO reacts with carbon and generates CO, resulting in a shift of the major reaction to SiO + CO with increasing p_{CO}/p_{CO_2} ratio, while aluminium remains in the molten fluorosilicate bath and eventually forms aluminium silicates. Under nitrogen gas, on the other hand, the evolved SiO gas reacts with nitrogen and carbon monoxide gases and forms powder O′-sialon phase when aluminium is present, while Si_2N_2O is a major phase if aluminium is absent.

The partial pressures of SiO, CO and CO_2 are estimated from the measured p_{O_2} and supersaturation ratio in the gas phase are compared for SiC and Si_3N_4 formation.

Acknowledgements

Financial support from the National Science Foundation through Grant MSM-8719951 is appreciated. Laboratory work of nitride reaction shown in Figs 4 and 7b by Dr M. J. Wang, and discussions by Dr T. Wada are appreciated.

References

1. H. WADA and M. J. WANG, in "Proceedings of the International Conference of Whisker- and Fiber-Toughened Composites", edited by R. A. Bradley *et al.* (ASM International, 1988) p. 63.
2. H. WADA, in "Proceedings of the International Symposium on Advances in Processing and Application of Ceramic and Metal Matrix Composites", edited by H. Mostaghaci (Pergamon Press, 1989) p. 3.
3. L. WANG and H. WADA, "Ceramic Powder Science", Vol. III, edited by G. H. Messing *et al.* (American Ceramic Society, 1990) p. 291.
4. M. J. WANG and H. WADA, *J. Mater. Sci.* **25** (1990) 1960.
5. H. WADA, in "Proceedings of the International Symposium on Advanced Structural Materials", edited by D. S. Wilkinson (Pergamon Press, 1988) p. 149.
6. M. J. WANG and H. WADA, *Mater. Sci. Forum* **47** (1989) 267.
7. J. V. MILEWSKI, F. D. GAC, J. J. PETROVIC and S. R. SKAGGS, *J. Mater. Sci.* **20** (1985) 1160.
8. H. SAITO, T. HAYASHI and K. MIURA, *J. Chem. Soc. Jpn* (1981) 1371.
9. *Idem., ibid.* (1982) 401.
10. T. HAYASHI, S. KAWABE and H. SAITO, *J. Ceram. Soc. Jpn* **95** (1986) 19.
11. T. MURAYAMA and H. WADA, in "Proceedings of Second International Symposium on Metallic Slag and Fluxes", edited by H. A. Fine and D. R. Gaskell (American Metallurgical Society, 1984) p. 135.
12. M. IWASE, E. ICHINOSE, N. YAMADA and K. NISHIDA, *Trans. Iron Steel Soc. AIME* **4** (1984) 47.
13. K. G. KING, W. O. WELLER and A. U. CHRISTENSEN, US Bureau of Mines, Special Report no. 5664 (1960).
14. C. B. ALCOCK and J. C. CHEN, *Canad. Metall. Q* **11** (1972) 559.
15. M. KATO and S. MINOWA, *Tetsu-to-Hagane* **55** (1969) 260.
16. A. HENDRY, in "Nitrogen Ceramics", edited by F. L. Reiley (Noordhoff International, 1977) p. 183.
17. K. H. JACK, *ibid.* p. 45.
18. I. COLQUHOUN, S. WILD, P. GRIEVESON and K. H. JACK, in "Proceedings 22, Ceramics for Turbines and Other High-Temperature Engineering Applications" (British Ceramic Society, 1973) p. 207.

19. S. WILD, P. GRIEVESON and K. H. JACK, in "Special Ceramics 5", edited by P. Popper (British Ceramic Society, 1972) p. 271.
20. H. WADA, M. J. WANG and T. Y. TIEN, *J. Amer. Ceram. Soc.* **71** (1988) 837.
21. "JANAF Thermochemical Tables", 3rd Edn (American Chemical Society, 1986).
22. J. J. BIERNACKI and G. P. WOTZAK, *J. Amer. Ceram. Soc.* **72** (1989) 122.
23. W. R. CANNON and S. C. ZHANG, in "Proceedings of the 3rd International Symposium on Ceramic Materials and Components for Engines", edited by V. J. Tennery (American Ceramic Society, 1989) p. 86.
24. J. G. LEE and I. B. CUTLER, in "Nitrogen Ceramics", edited by F. L. Reiley (Noordhoff International, 1977) p. 175.
25. M. MORI, H. INOUE and T. OCHIAI, *ibid*, p. 149.
26. H. WADA and M. J. WANG, presented at the Fall Meeting of Materials Research Society, Nov. 1990.

Received 7 November 1990
and accepted 10 April 1991